

1-1-2014

## Modelling the rejection of N-nitrosamines by a spiral-wound reverse osmosis system: mathematical model development and validation

Takahiro Fujioka  
*University of Wollongong, takahiro@uow.edu.au*

Stuart J. Khan  
*University of New South Wales, s.khan@unsw.edu.au*

James A. McDonald  
*University of New South Wales*

Annalie Roux  
*Seqwater*

Yvan Poussade  
*Veolia Water Australia, yvan.poussade@veoliawater.com.au*

*See next page for additional authors*

Follow this and additional works at: <https://ro.uow.edu.au/smartpapers>



Part of the [Engineering Commons](#), and the [Physical Sciences and Mathematics Commons](#)

---

### Recommended Citation

Fujioka, Takahiro; Khan, Stuart J.; McDonald, James A.; Roux, Annalie; Poussade, Yvan; Drewes, Jorg E.; and Nghiem, Long D., "Modelling the rejection of N-nitrosamines by a spiral-wound reverse osmosis system: mathematical model development and validation" (2014). *SMART Infrastructure Facility - Papers*. 116.  
<https://ro.uow.edu.au/smartpapers/116>

---

# Modelling the rejection of N-nitrosamines by a spiral-wound reverse osmosis system: mathematical model development and validation

## Abstract

A mathematical model was developed based on the irreversible thermodynamic principle and hydrodynamic calculation to predict the rejection of N-nitrosamines by spiral-wound reverse osmosis (RO) membrane systems. The developed model is able to accurately describe the rejection of N-nitrosamines under a range of permeate flux and system recovery conditions. The modelled N-nitrosamine rejections were in good agreement with values obtained experimentally using a pilot-scale RO filtration system. Simulation from the model revealed that an increase in permeate flux from 10 to 30 L/m<sup>2</sup>h led to an increase in the rejection of low molecular weight N-nitrosamines such as N-nitrosodimethylamine (NDMA) (from 31% to 54%), which was validated by experimental results. The modelling results also revealed that an increase in recovery caused a decrease in the rejection of these N-nitrosamines, which is consistent with the experimental results. Further modelling investigations suggested that NDMA rejection by a spiral-wound system can drop from 49% to 35% when the overall recovery increased from 10% to 50%. The model developed from this study can be a useful tool for water utilities and regulators for system design and evaluating the removal of N-nitrosamine by RO membranes.

## Keywords

reverse, validation, development, wound, spiral, nitrosamines, n, rejection, modelling, model, mathematical, system, osmosis

## Disciplines

Engineering | Physical Sciences and Mathematics

## Publication Details

Fujioka, T., Khan, S. J., McDonald, J. A., Roux, A., Poussade, Y., Drewes, J. E. & Nghiem, L. D. (2014). Modelling the rejection of N-nitrosamines by a spiral-wound reverse osmosis system: mathematical model development and validation. *Journal of Membrane Science*, 454 (March), 212-219.

## Authors

Takahiro Fujioka, Stuart J. Khan, James A. McDonald, Annalie Roux, Yvan Poussade, Jorg E. Drewes, and Long D. Nghiem

# **Modelling the rejection of N-nitrosamines by a Spiral-Wound Reverse Osmosis System: Mathematical model development and validation**

Revised Manuscript Submitted to

*Journal of Membrane Science*

Dec 2013

Takahiro Fujioka<sup>1</sup>, Stuart J. Khan<sup>2</sup>, James A. McDonald<sup>2</sup>, Annalie Roux<sup>3</sup>,  
Yvan Poussade<sup>4</sup>, and Jörg E. Drewes<sup>2,5</sup>, Long D. Nghiem<sup>1,\*</sup>

<sup>1</sup> Strategic Water Infrastructure Laboratory, School of Civil Mining and Environmental Engineering, The University of Wollongong, NSW 2522, Australia

<sup>2</sup> UNSW Water Research Centre, School of Civil and Environmental Engineering, The University of New South Wales, NSW 2052, Australia

<sup>3</sup> Seqwater, Level 2, 240 Margaret Street, Brisbane, QLD 4000, Australia

<sup>4</sup> Veolia Water Australia, Level 15, 127 Creek Street, Brisbane, QLD 4000, Australia

<sup>5</sup> Chair of Urban Water Systems Engineering, Technische Universität München, 85748 Garching, Germany

---

\* Corresponding author: Long Duc Nghiem, Email: longn@uow.edu.au, Ph +61 2 4221 4590

## **Abstract**

A mathematical model was developed based on the irreversible thermodynamic principle and hydrodynamic calculation to predict the rejection of N-nitrosamines by spiral-wound reverse osmosis (RO) membrane systems. The developed model is able to accurately describe the rejection of N-nitrosamines under a range of permeate flux and system recovery conditions. The modelled N-nitrosamine rejections were in good agreement with values obtained experimentally using a pilot-scale RO filtration system. Simulation from the model revealed that an increase in permeate flux from 10 to 30 L/m<sup>2</sup>h led to an increase in the rejection of low molecular weight N-nitrosamines such as N-nitrosodimethylamine (NDMA) (from 31 to 54%), which was validated by experimental results. The modelling results also revealed that an increase in recovery caused a decrease in the rejection of these N-nitrosamines, which is consistent with the experimental results. Further modelling investigations suggested that NDMA rejection by a spiral-wound system can drop from 49 to 35% when the overall recovery increased from 10 to 50%. The model developed from this study can be a useful tool for water utilities and regulators for system design and evaluating the removal of N-nitrosamine by RO membranes.

**Keywords:** Solute rejection modelling; NDMA; N-nitrosamines; reverse osmosis (RO); spiral-wound elements; water reuse.

## 1. Introduction

Augmenting potable water sources using reclaimed water is an important part of the water management portfolio in many regions of the world [1]. The planned use of reclaimed water to augment water supply is stringently regulated for the protection of public health. Thus, reclaimed water is commonly treated by a series of advanced treatment processes before being added to aquifers or reservoirs as the source of potable water supply. In many cases, these include reverse osmosis (RO) filtration to ensure the removal of pathogenic organisms, total dissolved solids and trace organic chemicals [1-4]. N-nitrosodimethylamine (NDMA) is one of several trace organic chemicals that are of particular concern due to its highly variable rejection efficiency by RO membranes as reported in several recent pilot- and full-scale studies [5-7]. NDMA is a disinfection by-product formed during the chloramination of biologically treated effluent [8] and is often found in the RO feed at up to a few hundred parts per trillion [9]. In addition to NDMA, other N-nitrosamines that are often present in raw wastewater and secondary treated effluents including N-nitrosomethylethylamine (NMEA), N-nitrosopyrrolidine (NPYR), N-nitrosodiethylamine (NDEA), N-nitrosopiperidine (NPIP), N-nitrosomorpholine (NMOR), N-nitrosodipropylamine (NDPA) and N-nitrosodibutylamine (NDBA) [10-12]. Several of these N-nitrosamines (including NDMA) have been classified as probable human carcinogens by the US EPA [13]. Thus, their concentrations in drinking water have been regulated by regulatory authorities around the world. For examples, the Australian Guidelines for Water Recycling have recommended their concentrations at 10 ng/L (NDMA and NDEA) and at 1 ng/L (NMOR) for the augmentation of drinking water sources [14].

Modelling the rejection of N-nitrosamines under various conditions is essential for the design of RO plants and compliance monitoring. NDMA and several other N-nitrosamines have been frequently detected in the feed water to RO treatment at concentration higher than the regulatory levels [15]. In addition, N-nitrosamine rejection by RO membranes is sensitive to operating conditions and feed solution characteristics [16]. Difficulties associated with analytical determination of N-nitrosamines in the permeate at regulatory concentrations (i.e. 1 to 10 ng/L) [5, 17, 18] also underscore the need for a model that can accurately describe the rejection of N-nitrosamines. N-nitrosamine concentrations in aqueous samples can be determined by chromatography (GC) or high pressure liquid chromatography (HPLC) with

tandem mass spectrometry (MS/MS) detector. However, the number of commercial laboratories capable of trace level N-nitrosamine analysis is still limited and regular monitoring of N-nitrosamines remains difficult and expensive. Thus, a capacity to describe and predict the rejection of N-nitrosamines by the RO process is particularly useful for the management of these trace organic chemicals in water recycling applications.

The rejection of inorganic salts by multi-stage RO membrane systems can be simulated with a high level of accuracy using commercially available RO design software packages (e.g. IMSDesign, TorayDS/DS2, and ROSA provided by Hydranautics, Toray, and Dow/FilmTec, respectively). The development of mathematical models for simulating specific trace organic and inorganic chemicals by spiral wound RO membrane systems has been reported in several recent studies. Kim and co-workers have successfully developed a model for predicting boron rejection by applying the irreversible thermodynamic principle and sub-dividing a spiral wound element into a number of small sub-sections [19-21]. Using a similar approach, Verliefde et al. [22] have also developed a full-scale rejection model for several pharmaceutically active compounds (PhACs) using nanofiltration (NF) membranes. These models significantly enhance our understanding of the permeation of boron and PhACs through RO membranes under realistic conditions. However, to date, there have yet been any software packages or mathematical models that can simulate the rejection of N-nitrosamines.

The aim of this study was to develop a mathematical model to predict the rejection of N-nitrosamines by RO systems under a range of operating conditions. The developed model was validated using experimental data obtained from a pilot RO system. The potential application of this model for predicting N-nitrosamine rejection at full-scale level was also discussed.

## **2. Theoretical background**

### *2.1. Membrane element characteristics*

A commercial spiral-wound element has one or several membrane leaves. Each leaf consists of two flat sheet membranes sealed on three sides with the fourth side attached to a perforated tube called the permeate collector. The membrane leaf is wound around the permeate collector. As a result, each spiral-wound element can essentially be presented by a large flat sheet membrane. In this study, each element is geometrically described with the length ( $L$ ),

width ( $W$ ) and feed channel height ( $h_b$ ) (Figure 1). On the other hand, the irreversible thermodynamic principle can be used to model the rejection of N-nitrosamines by a small flat sheet membrane for a given hydrodynamic condition. Thus, the irreversible thermodynamic principle can also be used to model solute rejection by a spiral wound element. This can be done by sub-dividing the membrane area on each element smaller sections of the same size and using fluid mechanics to calculate and define the hydrodynamic condition for each sub-section. In this study, the membrane area on one each element is divided into 20 sub-sections ( $m = 20$ ) in a longitudinal direction where each sub-section length ( $\Delta x$ ) is described as:

$$\Delta x = \frac{L}{m} \quad (1)$$

It is noteworthy that the length of each sub-section selected here is similar to that of the flat sheet membrane coupon used in the laboratory-scale study. The membrane surface area attached to the feed spacers is assumed to be 10% and this area is not utilised for filtration. Thus, the active surface area in each sub-section ( $\Delta S$ ) is defined as:

$$\Delta S = \frac{0.9S}{m} \quad (2)$$

The cross-section area of the feed channel ( $\Delta S_c$ ) is expressed as:

$$\Delta S_c = Wh_b \quad (3)$$

**[Figure 1]**

## 2.2. Hydrodynamics

The local permeate flux ( $J_p(i)$ ), local permeate flow rate ( $Q_p(i)$ ) and the overall permeate flow rate of a membrane element ( $Q_{p,t}$ ) are calculated using equations 4 - 6.

$$J_p(i) = L_p \left( \{P_f(i) - P_p(i)\} - \sigma \Delta \pi(i) \right) \quad (4)$$

$$Q_p(i) = J_p(i) \times \Delta S \quad (5)$$

$$Q_{p,t} = \sum_{i=1}^m Q_p(i) \quad (6)$$

where  $L_p$  = pure water permeability which is obtained from bench-scale tests and  $\sigma$  = reflection coefficient. Because permeate pressure ( $P_p$ ) is negligible compared to feed pressure ( $P_f$ ), local permeate pressure ( $P_p(i)$ ) is assumed to be zero in this study. Local osmotic pressure ( $\pi(i)$ ) shown in equation 4 is computed with feed solution temperature ( $T$ ) and molar concentrations of ions ( $m_{salt}(i)$ ).

$$\pi(i) = 1.19(T + 273) \sum_1^i m(i) \quad (7)$$

Concentration of the solute ( $m_{salt}(i)$ ) increases in the feed in the subsequent sub-sections since the solute is retained by the membrane. Changes in solute concentration can be calculated using the following equation:

$$m_{salt}(i+1) = m_{salt}(i) \frac{Q_f(i) - (1 - R_{salt}) \times Q_p(i)}{Q_f(i+1)} \quad (8)$$

where  $Q_f(i)$  = local feed flow rate. In the model, overall feed flow measured in the pilot system is used as the feed flow of the first sub-section  $Q_f(1)$ . Local feed flow rate ( $Q_f(i+1)$ ) is calculated from the feed and permeate flow rates of the previous sub-section ( $Q_f(i)$ ):

$$Q_f(i+1) = Q_f(i) - Q_p(i) \quad (9)$$

Using the local feed flow rate ( $Q_f(i)$ ), local bulk velocity of the feed within the feed channel ( $U_b(i)$ ) is defined as:

$$U_b(i) = \frac{Q_f(i)}{\Delta S_c} \quad (10)$$

The pressure drop in the feed stream ( $\Delta P_f(i)$ ) and overall pressure drop of an element in the feed stream ( $\Delta P_{ft}$ ) is calculated using the following formula [23, 24]:

$$\Delta P_f(i) = \frac{1}{2} f_{fb} \rho(i) U_b^2(i) \frac{\Delta x}{d_h} \quad (11)$$

$$\rho(i) = 498.4M + \sqrt{248400 M^2 + 752.4M \Sigma C_{salt}} \quad (12)$$



$$M = 1.0069 - 2.757 \times 10^{-4} T \quad (13)$$

$$\Delta P_{f,t} = \sum_{i=1}^m \Delta P_f(i) \quad (14)$$

where  $f_{fb}$  = feed friction parameter,  $\rho(i)$  = local solution density [25],  $T$  = feed temperature and  $d_h$  = hydraulic diameter ( $d_h = 2h_b$ ) [23]. Friction parameter ( $f_{fb}$ ) is determined by an approach minimising the difference between the experimentally modelled and measured overall pressure drops. Feed pressure which is experimentally measured at the entrance of the first membrane element is used as the feed pressure of the first sub-section in the model. Then local feed pressure ( $P_f(i+1)$ ) is calculated from the feed pressure ( $P_f(i)$ ) and the feed pressure loss ( $\Delta P_f(i)$ ) of the previous section:

$$P_f(i+1) = P_f(i) - \Delta P_f(i) \quad (15)$$

**[Figure 2]**

### 2.3. Solute permeation through membranes

Local real rejection ( $R_{real}(i)$ ) of various solutes such as ions and organic chemicals including N-nitrosamines [26-29] can be commonly expressed by the Spiegler-Kedem equation [30]:

$$R_{real}(i) = 1 - \frac{C_p(i)}{C_m(i)} = \frac{\sigma(1-F(i))}{(1-\sigma F(i))} \quad (16)$$

$$F(i) = \exp\left(-\frac{(1-\sigma)}{P_s} J_p(i)\right) \quad (17)$$

where  $P_s$  = permeability coefficient and  $\sigma$  = reflection coefficient both of which can be obtained from bench-scale experiments. Local observed rejection ( $R_{obs}(i)$ ) can be calculated with the local real rejection ( $R_{real}(i)$ ) and local mass transfer coefficient ( $k(i)$ ) as follows [31]:

$$R_{obs}(i) = \frac{R_{real}(i)}{(1 - R_{real}(i)) \times \exp\left(\frac{J_p(i)}{k(i)}\right) + R_{real}(i)} \quad (18)$$

$$k(i) = 0.753 \left( \frac{K}{2-K} \right)^{0.5} \left( \frac{D}{h_b} \right) Sc(i)^{-1/6} \left( \frac{Pe h_b}{\Delta L} \right)^{0.5} \quad (19)$$

where  $K$  = efficiency of mixing net ( $K = 0.5$ ),  $Sc$  = Schmidt number ( $\mu/\rho(i)D$ ),  $Pe$  = Peclet number ( $Pe = 2h_b U_b(i)/D$ ) and  $\mu$  = viscosity of feed solution.

$$\mu = 2.141 \times 10^{-5} \times 10^{\frac{247.8}{T-140}} \quad (20)$$

Once the local observed rejection ( $R_{obs}(i)$ ) is determined, the local permeate concentration ( $C_p(i)$ ) can also be calculated using local feed concentration ( $C_f(i)$ ) using equation 21. Then local feed concentration in the following sub-section ( $C_f(i+1)$ ) can be expressed by equation 22. The overall permeate concentration of an element  $j$  ( $C_p(j)$ ) can be calculated by totalling mass transport in all sub-sections of the membrane element as described in equation 23.

$$C_p(i) = C_f(i)(1 - R_{obs}(i)) \quad (21)$$

$$C_f(i+1) = \frac{Q_f(i)C_f(i) - Q_p(i)C_p(i)}{Q_c(i)} \quad (22)$$

$$C_p(j) = \frac{\sum_{i=1}^m C_p(i)Q_p(i)}{\sum_{i=1}^m Q_p(i)} \quad (23)$$

Because permeate streams from each membrane element blend in the combined permeate stream, solute rejection by a certain number ( $n$ ) of membrane elements need to be evaluated using the combined concentration. The combined permeate concentration of  $n$  elements ( $C_p(n)$ ), combined observed solute rejection of  $n$  elements ( $R_{obs}(n)$ ), and recovery of  $n$  elements ( $R_c(n)$ ) can be calculated as follows:

$$C_p(n) = \frac{\sum_{j=1}^n C_p(j)Q_p(j)}{\sum_{j=1}^n Q_p(j)} \quad (24)$$

$$R_{obs}(n) = \frac{C_f(j) - C_p(n)}{C_f(j)}, \quad j = 1 \quad (25)$$

$$R_c(n) = \frac{\sum_{j=1}^n Q_p(j)}{Q_f(j)}, \quad j = 1 \quad (26)$$

The iterative procedure to determine the hydrodynamic constants (Eqs 1 – 15) and solute transport following the irreversible thermodynamic principle described Eqs 16 – 26 above provide the basis for this mathematical model as schematically summarised in Figure 2.

### 3. Materials and methods

#### 3.1. Pilot-scale filtration system and RO element

A pilot-scale cross-flow RO filtration system was used in this investigation. The pilot system comprises three 4 inch glass-fibre pressure vessels, 300 L feed reservoir, stainless steel pipes in the feed stream and PVC pipes in the permeate stream (Figure 3). Each pressure vessel holds one 4 inch  $\times$  40 inch RO membrane element. The feed solution was delivered from the feed reservoir to the first stage by a pump (CRN 3-25, Grundfos, Bjerringbro, Denmark) and the concentrate of the first stage was transferred to the second stage followed by the third stage. The permeate and concentrate streams were returned back into the feed reservoir. The permeate flow rate and cross flow rate were both monitored by flow meters and regulated by a globe valve and speed controller of the pump. Feed solution temperature was conditioned in the feed reservoir using stainless steel heat exchanging pipes connected to a chillier/heater unit (Aqua Cooler S360PD-CT, Chester Hill, NSW, Australia).

#### [Figure 3]

Three ESPA2-4040 (Hydranautics, Oceanside, CA, USA) spiral wound elements were used. The ESPA2-4040 membrane element has an equivalent length of 1.016 m, actual membrane sheet length ( $L$ ) of 0.9 m, membrane area ( $S$ ) of 7.9 m<sup>2</sup>, and feed channel height ( $h_b$ ) of  $6.60 \times 10^{-4}$  m. According to the manufacturer, permeability of individual membrane element may vary by up to 25%. It is noteworthy that the ESPA2 membrane is commonly deployed in full-scale RO installations in the USA and Australia for water reuse application [5, 32].

### 3.2. Chemicals

Analytical grade N-nitrosamines were obtained from by Sigma-Aldrich (St Louis, MO, USA). An N-nitrosamine stock solution containing 10 mg/L of each N-nitrosamine was prepared in pure methanol. All N-nitrosamines used in this investigation exist as an uncharged solute in treated wastewater (pH 6-8) [16]. Deuterated N-nitrosamines (N-nitrosodimethylamine-D6, N-nitrosomethylethylamine-D3, N-nitrosopyrrolidine-D8, N-nitrosodiethylamine-D10, N-nitrosopiperidine-D10, N-nitrosomorpholine-D8, N-nitrosodipropylamine-D14 and N-nitrosodi-n-butylamine-D9) were supplied by CDN isotopes (Pointe-Claire, Quebec, Canada) and a surrogate stock solution of 100 µg/L of each deuterated N-nitrosamine was also prepared in pure methanol. These stock solutions were kept at -18 °C in the dark and were used within 1 month of preparation. Key physicochemical properties and transport parameters of these N-nitrosamines through the ESPA2 membrane which was obtained from a previous study [33] are summarised in Table 1. Analytical grade NaCl, CaCl<sub>2</sub> and NaHCO<sub>3</sub> were also purchased from Ajax Finechem (Taren Point, NSW, Australia). Stock solutions of these chemicals were also prepared in Milli-Q water at 2M (NaCl) and 0.1M (CaCl<sub>2</sub> and NaHCO<sub>3</sub>) concentrations and used as the background electrolytes during the filtration experiments.

[Table 1]

### 3.3. Filtration experiments

Prior to the first filtration experiment, the membrane system was operated at approximately 1000 kPa for 12 hours using 100 L Milli-Q water. Following the start-up stage, the Milli-Q water in the feed was conditioned with 20 mM NaCl, 1 mM CaCl<sub>2</sub> and 1 mM NaHCO<sub>3</sub> to simulate the background electrolyte composition typically found in treated wastewater. The stock solution of N-nitrosamines was also introduced into the feed to obtain approximately 250 ng/L of each N-nitrosamine. The permeate flux was then adjusted to 10 L/m<sup>2</sup>h, and stepwise increased up to 30 L/m<sup>2</sup>h. The overall system recovery was adjusted to 25% because only three membrane elements were used. During the experiments, feed pressure was measured at the entrance of the each element and the exit of the third element. The system was operated for at the least 12 h before the first samples were taken for analysis to ensure the separation efficiency has been stabilised. A previous laboratory-scale study revealed no significant changes in the rejection of almost all N-nitrosamines after one hour of filtration

[16]. From each sampling point, a sample of 200 mL was collected using amber glass bottles for N-nitrosamine analysis. Immediately after the sample collection, the surrogate stock solution was added to the sampling bottles to obtain 50 ng/L of each isotope labelled N-nitrosamine. The feed temperature during the experiments was kept at  $20\pm 0.1^\circ\text{C}$ . It is noteworthy that the overall recovery of each vessel (or stage) which holds six to seven RO elements is about 50% in most full-scale wastewater recycling RO plants.

### *3.4. Analytical technique*

N-nitrosamine concentrations were determined using an analytical method previously developed by McDonald et al. [18]. The method uses solid phase extraction (SPE), followed by gas chromatography and analysis by tandem mass spectrometry with electron impact ionization. SPE was conducted using Supelclean<sup>TM</sup> Coconut Charcoal SPE cartridges purchased from Supelco (St Louis, MO, USA). The concentrations of N-nitrosamines were quantified using an Agilent 7890A gas chromatograph coupled with an Agilent 7000B triple quadrupole mass spectrometer. Calibration curves were established for each N-nitrosamine with a range of 0.5-500 ng/L. The quantitative detection limits established in this investigation were 3 ng/L for NDMA, NDEA, NPIP, and NMOR, and 5 ng/L for NMEA, NPYR, NDPA, and NDBA. Conductivity and pH were measured using an Orion 4-Star Plus pH/conductivity meter (Thermo Scientific, USA).

## **4. Results and discussion**

### *4.1. Determination of model parameters*

The pressure of each sub-section within the membrane system was calculated from the pressure of the previous sub-section and the local pressure drop. The local pressure drop ( $\Delta P(i)$ ) was determined using equation 11. The feed friction parameter ( $f_{fb}$ ), which is dependent upon the geometry of membrane element and operating conditions [23, 24], was obtained using the iteration procedure outline in Figure 2 to minimise the difference between the modelled and observed feed pressure to less than 5% at an average permeate flux of 10, 20, and 30  $\text{Lm}^2/\text{h}$  (Figure 4). In this study,  $f_{fb}$  values of 10, 20 and 30  $\text{Lm}^2/\text{h}$  were 3.9, 4.3 and 5.5, respectively. Knowing the membrane permeability, the local permeate flux can then be calculated based on the local pressure. Subsequently, the overall permeate flux can also be calculated. In fact, the simulated permeate flux only deviated slightly from the observed

value at the applied pressure of 1.0 MPa (Figure 5). These results indicate that the model can adequately simulate the hydrodynamic condition (i.e. feed pressure and permeate flow) within the RO membrane elements. The small deviation observed in Figure 5 may be attributed to the fact that the determined  $f_{fb}$  value was used for the entire system as well as the difference in permeability of membranes that were used in the fundamental and pilot-scale experiments. There can be some variation in permeability between different areas of the same membrane element or between different batches of production (Section 3.1). As the applied pressure increases, the pressure drop across the membrane element increases resulting in a larger deviation between the simulated and experimentally obtained values.

[Figure 4]

[Figure 5]

#### 4.2. *N*-nitrosamine rejection

All *N*-nitrosamines used in this study are uncharged in the tested solution (pH 8). In general, the rejection of uncharged solutes by NF/RO membranes generally increases as permeate flux increases [22]. A similar trend using *N*-nitrosamines was also reported in a previous laboratory-scale study by Fujioka et al. [16]. As expected, the simulated rejection values of three lowest molecular weight *N*-nitrosamines (i.e. NDMA, NMEA and NPYR) increased when the overall (system) permeate flux increased (Figure 6). Among these three *N*-nitrosamines, modelled NDMA rejection showed the most significant increase from 31 to 54% with increasing overall permeate flux from 10 to 30 L/m<sup>2</sup>h, respectively. The impact of permeate flux on *N*-nitrosamine rejection was less significant as their molecular weights increase. The modelled rejections were comparable with the observed rejections at three different overall permeate fluxes (i.e. 10, 20 and 30 L/m<sup>2</sup>h) investigated here. Results from Figure 6 indicate that the developed model is capable of describing *N*-nitrosamine rejection at a range of permeate flux. It is also noteworthy that rejection values obtained from the model are conservative. In other word, the modelled rejections of NDMA, NMEA, and NPYR were slightly smaller than values obtained experimentally.

Modelled rejections of the other *N*-nitrosamines (i.e. NDEA, NPIP, NDPA, NMOR and NDBA) were over 90%. As a result, only a slight increase in rejection was found with increasing overall permeate flux (data not shown). In fact, pilot-scale experiments conducted

in this study revealed that the observed rejections of these N-nitrosamines were over 90% and no discernible variation in rejection was observed for changes in permeate flux (Figure 7).

**[Figure 6]**

**[Figure 7]**

#### *4.3. Impact of recoveries*

In full-scale RO plants, solute rejection can vary depending on the element position within a vessel and the overall train due to changes in hydrodynamic states and solution characteristics. The variation in solute rejection was investigated by extending the model calculation from three elements to seven elements and the rejections were plotted against recovery (Figure 8). The model showed approximately 50% recovery with seven RO membrane elements, which is equivalent to one vessel of the first stage in a full-scale RO train deployed for water reclamation applications. The simulated rejections of the three N-nitrosamines decreased when recovery increased (Figure 8). When the recovery of the RO system increased from 10 to 50%, the modelled rejection of NDMA decreased remarkably from 49 to 35%. Likewise, for the same change in recovery, the rejections of NMEA and NPYR also decreased from 81 to 72% and from 89 to 83%, respectively. The observed rejections of these three N-nitrosamines were similar to the modelled rejections (Figure 8).

**[Figure 8]**

Changes in the localised rejection of NDMA within a membrane vessel containing several elements were further investigated by examining the variation in hydrodynamic states and mass transfers. As filtration progresses, local feed pressure decreases due to an increase in pressure loss (Figure 9). As a result of the reduced driving force, local permeate flux decreases along with the progress of the filtration. Since permeate flux affects the rejection of N-nitrosamines [33], the local NDMA rejection could also decrease. It is also noteworthy that an increase in TDS along with filtration also causes a slight decrease in N-nitrosamine rejection [33]. In addition, rejected compounds remain in the feed stream, leading to an increase in NDMA concentration in the subsequent feed and permeate. The increased NDMA concentration in the permeate stream contributes to deteriorations in the overall rejection of solutes, since the overall rejection is calculated based on solute concentrations in the feed

solution and combined permeate solution as described in equation 25. Thus, the simulation results reported here could explain the discrepancy between laboratory scale results with very low recovery and those from full-scale RO plants for water recycling applications with about 85% recovery [15].

[Figure 9]

## 5. Conclusions

The developed model successfully simulated the hydrodynamic states (i.e. pressure and permeate flow) of the pilot-scale plant. The modelled results revealed that changes in permeate flux (from 10 to 30 L/m<sup>2</sup>h) considerably affected the rejection of low molecular weight N-nitrosamines such as NDMA (from 31 to 54%). The modelled N-nitrosamine rejections at each permeate flux were in a good agreement with experimentally determined N-nitrosamine rejections. Modelling conditions simulating a vessel with seven spiral-wound membrane elements revealed that recovery plays an important role in the rejection of low-molecular weight N-nitrosamines. In particular, when recovery changed from 10 to 50% by increasing the number of elements from one to seven, NDMA rejection decreased considerably from 49 to 35%. Additional simulation using the model revealed that the local NDMA rejection decreased with NDMA concentration increasing along the flow path from the first to the last stage, resulting in a decrease in the overall rejection of NDMA. The presented results demonstrate that the developed model can be used for simulating N-nitrosamine rejections during full-scale plant design and operation. Further work is required to examine the effects of several other factors (e.g. feed water characteristics, fouling and chemical cleaning) on N-nitrosamine rejection using a pilot-scale plant and incorporate these effects into the model.

## 6. Acknowledgements

This work was supported by the Australian Research Council Linkage Projects LP0990705 (with industry support from Veolia Water and Seqwater). The authors acknowledge the University of Wollongong for a PhD scholarship awarded to Takahiro Fujioka.

## 7. Nomenclature

$C_f$  feed concentration [kg/m<sup>3</sup>]



$C_p$	permeate concentration [kg/m <sup>3</sup> ]
$h_b$	feed channel height [m]
$i$	number of sub-section [-]
$j$	number of element [-]
$f_{fb}$	feed friction parameter [-]
$J_p$	permeate flux [m <sup>3</sup> /m <sup>2</sup> s]
$k$	mass transfer coefficient [m/s]
$K$	efficiency of mixing net [-]
$L$	membrane sheet length [m]
$L_p$	pure water permeability [L/m <sup>2</sup> hPa]
$m$	number of sub-sections in a membrane sheet [-]
$m_{salt}$	molar concentrations of ions [mol/L]
$n$	quantity of elements [-]
Pe	Peclet number [-]
$P_f$	feed pressure [Pa]
$P_p$	feed pressure [Pa]
$\Delta P$	pressure drop [Pa]
$P_s$	permeability coefficient of a compound [m/s]
$Q_f$	feed flow [m <sup>3</sup> /s]
$Q_p$	permeate flow [m <sup>3</sup> /s]
$R_c$	recovery [-]
$R_{obs}$	observed rejection [-]
$R_{real}$	real rejection [-]
$\Delta S$	valid surface area [m]

$\Delta S_c$	cross-section area [m]
$Sc$	Schmidt number [-]
$T$	feed solution temperature [ $^{\circ}C$ ]
$U_b$	bulk velocity of the feed within the feed channel [m/s]
$W$	membrane sheet width [m]
$\Delta x$	sub-section length [m]
$\rho$	density of solution [ $kg/m^3$ ]
$\sigma$	reflection coefficient [-]
$\pi$	osmotic pressure [Pa]
$\mu$	viscosity of feed solution [Pa-s]

## 8. References

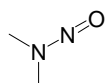
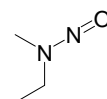
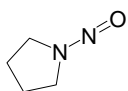
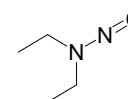
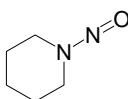
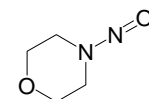
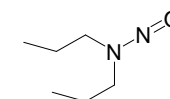
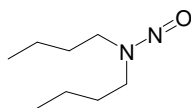
- [1] M.A. Shannon, P.W. Bohn, M. Elimelech, J.G. Georgiadis, B.J. Marinas, A.M. Mayes, Science and technology for water purification in the coming decades, *Nature*, 452 (2008) 301-310.
- [2] C. Bellona, J.E. Drewes, P. Xu, G. Amy, Factors affecting the rejection of organic solutes during NF/RO treatment - A literature review, *Water Res.*, 38 (2004) 2795-2809.
- [3] A.R.D. Verliefe, S.G.J. Heijman, E.R. Cornelissen, G.L. Amy, B. Van der Bruggen, J.C. van Dijk, Rejection of trace organic pollutants with high pressure membranes (NF/RO), *Environ. Prog.*, 27 (2008) 180-188.
- [4] G. Oron, L. Gillerman, A. Bick, N. Buriakovsky, Y. Manor, E. Ben-Yitshak, L. Katz, J. Hagin, A two stage membrane treatment of secondary effluent for unrestricted reuse and sustainable agricultural production, *Desalination*, 187 (2006) 335-345.
- [5] M.H. Plumlee, M. López-Mesas, A. Heidlberger, K.P. Ishida, M. Reinhard, N-nitrosodimethylamine (NDMA) removal by reverse osmosis and UV treatment and analysis via LC-MS/MS, *Water Res.*, 42 (2008) 347-355.
- [6] M.J. Farré, K. Döderer, L. Hearn, Y. Poussade, J. Keller, W. Gernjak, Understanding the operational parameters affecting NDMA formation at Advanced Water Treatment Plants, *J. Hazard. Mater.*, 185 (2011) 1575-1581.
- [7] S.J. Khan, J.A. McDonald, Quantifying human exposure to contaminants for multiple-barrier water reuse systems, *Water Sci. Technol.*, 61 (2010) 77-83.

- [8] W.A. Mitch, J.O. Sharp, R.R. Trussell, R.L. Valentine, L. Alvarez-Cohen, D.L. Sedlak, N-Nitrosodimethylamine (NDMA) as a drinking water contaminant: A review, *Environ. Eng. Sci.*, 20 (2003) 389-404.
- [9] S.W. Krasner, P. Westerhoff, B. Chen, B.E. Rittmann, G. Amy, Occurrence of disinfection byproducts in United States wastewater treatment plant effluents, *Environ. Sci. Technol.*, 43 (2009) 8320-8325.
- [10] M. Krauss, P. Longrée, E. van Houtte, J. Cauwenberghs, J. Hollender, Assessing the fate of Nitrosamine precursors in wastewater treatment by physicochemical fractionation, *Environ. Sci. Technol.*, 44 (2010) 7871-7877.
- [11] C. Reyes-Contreras, C. Domínguez, J.M. Bayona, Determination of nitrosamines and caffeine metabolites in wastewaters using gas chromatography mass spectrometry and ionic liquid stationary phases, *J. Chromatogr. A*, 1261 (2012) 164-170.
- [12] S. Yoon, N. Nakada, H. Tanaka, A new method for quantifying N-nitrosamines in wastewater samples by gas chromatography—triple quadrupole mass spectrometry, *Talanta*, 97 (2012) 256-261.
- [13] USEPA, N-Nitrosodimethylamine (CASRN 62-75-9) - Integrated risk information system (IRIS), <http://www.epa.gov/iris/subst/0045.htm> (1993).
- [14] NRMMC, EPHC, AHMC, Australian guidelines for water recycling: Managing health and environmental risks (Phase 2): Augmentation of drinking water supplies, Environment Protection and Heritage Council, National Health and Medical Research Council, Natural Resource Management Ministerial Council, Canberra, 2008.
- [15] T. Fujioka, S.J. Khan, Y. Poussade, J.E. Drewes, L.D. Nghiem, N-nitrosamine removal by reverse osmosis for indirect potable water reuse – A critical review based on observations from laboratory-, pilot- and full-scale studies, *Sep. Purif. Technol.*, 98 (2012) 503-515.
- [16] T. Fujioka, L.D. Nghiem, S.J. Khan, J.A. McDonald, Y. Poussade, J.E. Drewes, Effects of feed solution characteristics on the rejection of N-nitrosamines by reverse osmosis membranes, *J. Membr. Sci.*, 409–410 (2012) 66-74.
- [17] J.W. Munch, M.V. Bassett, METHOD 521 Determination of nitrosamines in drinking water by solid phase extraction and capillary column gas chromatography with large volume injection and chemical ionization tandem mass spectrometry (MS/MS) Version 1.0, in, National Exposure Research Laboratory Office of Research and Development, U.S. Environmental Protection Agency, Cincinnati, 2004.
- [18] J.A. McDonald, N.B. Harden, L.D. Nghiem, S.J. Khan, Analysis of N-nitrosamines in water by isotope dilution gas chromatography-electron ionisation tandem mass spectrometry, *Talanta*, 99 (2012) 146-152.
- [19] P.P. Mane, P.-K. Park, H. Hyung, J.C. Brown, J.-H. Kim, Modeling boron rejection in pilot- and full-scale reverse osmosis desalination processes, *J. Membr. Sci.*, 338 (2009) 119-127.

- [20] P.-K. Park, S. Lee, J.-S. Cho, J.-H. Kim, Full-scale simulation of seawater reverse osmosis desalination processes for boron removal: Effect of membrane fouling, *Water Res.*, 46 (2012) 3796-3804.
- [21] H. Hyung, J.-H. Kim, A mechanistic study on boron rejection by sea water reverse osmosis membranes, *J. Membr. Sci.*, 286 (2006) 269-278.
- [22] A.R.D. Verliefde, E.R. Cornelissen, S.G.J. Heijman, J.Q.J.C. Verberk, G.L. Amy, B. Van der Bruggen, J.C. van Dijk, Construction and validation of a full-scale model for rejection of organic micropollutants by NF membranes, *J. Membr. Sci.*, 339 (2009) 10-20.
- [23] G. Schock, A. Miquel, Mass transfer and pressure loss in spiral wound modules, *Desalination*, 64 (1987) 339-352.
- [24] E.M.V. Hoek, J. Allred, T. Knoell, B.-H. Jeong, Modeling the effects of fouling on full-scale reverse osmosis processes, *J. Membr. Sci.*, 314 (2008) 33-49.
- [25] K.M. Sassi, I.M. Mujtaba, Effective design of reverse osmosis based desalination process considering wide range of salinity and seawater temperature, *Desalination*, 306 (2012) 8-16.
- [26] Y. Miyashita, S.-H. Park, H. Hyung, C.-H. Huang, J.-H. Kim, Removal of N-Nitrosamines and their precursors by nanofiltration and reverse osmosis membranes, *J. Environ. Eng.*, 135 (2009) 788-795.
- [27] C. Bellona, K. Budgell, D. Ball, K. Spangler, J.E. Drewes, S. Chellam, Models to predict organic contaminant removal by RO and NF membranes, *IDA Journal*, 3 (2011) 40-44.
- [28] T. Tsuru, K. Ogawa, M. Kanezashi, T. Yoshioka, Permeation characteristics of electrolytes and neutral solutes through titania nanofiltration membranes at high temperatures, *Langmuir*, 26 (2010) 10897-10905.
- [29] T. Tsuru, S. Izumi, T. Yoshioka, M. Asaeda, Temperature effect on transport performance by inorganic nanofiltration membranes, *AIChE Journal*, 46 (2000) 565-574.
- [30] O. Kedem, A. Katchalsky, Permeability of composite membranes. Part 1.-Electric current, volume flow and flow of solute through membranes, *Trans. Faraday Soc.*, 59 (1963) 1918-1930.
- [31] S. Senthilmurugan, A. Ahluwalia, S.K. Gupta, Modeling of a spiral-wound module and estimation of model parameters using numerical techniques, *Desalination*, 173 (2005) 269-286.
- [32] M.J. Farré, J. Keller, N. Holling, Y. Poussade, W. Gernjak, Occurrence of NDMA precursors in wastewater treatment plant effluent and their fate during UF-RO membrane treatment, *Water Sci. Technol.*, 63 (2011) 605-612.

- [33] T. Fujioka, S.J. Khan, J.A. McDonald, A. Roux, Y. Poussade, J.E. Drewes, L.D. Nghiem, N-nitrosamine rejection by nanofiltration and reverse osmosis membranes: The importance of membrane characteristics, *Desalination*, 316 (2013) 67-75.

486 **Table 1:** Physicochemical characteristics and transport parameters of the selected N-nitrosamines.

Name	NDMA	NMEA	NPYR	NDEA	NPIP	NMOR	NDPA	NDBA
Structure								
Molecular weight [g/mol]	74.05	88.06	100.06	102.08	114.08	116.06	130.11	158.14
Log $K_{ow}$ <sup>a</sup>	-0.50	0.01	-0.09	0.52	0.44	-0.81	1.54	2.56
Diffusion coefficient <sup>b</sup> , $D$ [m <sup>2</sup> /s]	$9.7 \times 10^{-10}$	$8.0 \times 10^{-10}$	$8.0 \times 10^{-10}$	$8.0 \times 10^{-10}$	$8.6 \times 10^{-10}$	$9.2 \times 10^{-10}$	$8.2 \times 10^{-10}$	$8.0 \times 10^{-10}$
Permeability coefficient <sup>c</sup> , $P_s$ [m/s]	$5.35 \times 10^{-6}$	$1.14 \times 10^{-6}$	$5.12 \times 10^{-7}$	$2.26 \times 10^{-7}$	$9.25 \times 10^{-8}$	$2.06 \times 10^{-7}$	$6.02 \times 10^{-8}$	$4.33 \times 10^{-8}$
Reflection coefficient <sup>c</sup> , $\sigma$ [-]	0.953	0.958	0.973	0.985	0.993	0.991	0.992	0.990

487 <sup>a</sup> ACD/PhysChem Suite software (Advanced Chemistry Development, Inc., Ontario, Canada).

488 <sup>b</sup> GSI chemical properties database (GSI Environmental Inc.), <http://www.gsi-net.com/en/publications/gsi-chemical-database.html>.

489 <sup>c</sup> [33].

490 **LIST OF FIGURES**

491 **Figure 1:** Representation of a spiral-wound RO element as flat sheet configuration including  
492 the mass balance of a flat sheet sub-section.

493 **Figure 2:** Schematic diagram of the iteration procedure to determine the pressure drop in a  
494 spiral-wound element and the subsequent rejection calculation.

495 **Figure 3:** Flow diagram of the pilot-scale plant.

496 **Figure 4:** Observed and modelled feed pressure within three RO elements (overall permeate  
497 flux = 10, 20 and 30 L/m<sup>2</sup>h; feed solution contains 20 mM NaCl, 1 mM NaHCO<sub>3</sub>, and 1 mM  
498 CaCl<sub>2</sub>; feed temperature = 20.0 ± 0.1 °C).

499 **Figure 5:** Observed and modelled overall permeate flux as a function of the feed pressure at  
500 the system entrance (feed solution contains 20 mM NaCl, 1 mM NaHCO<sub>3</sub>, and 1 mM CaCl<sub>2</sub>;  
501 feed temperature = 20.0 ± 0.1 °C).

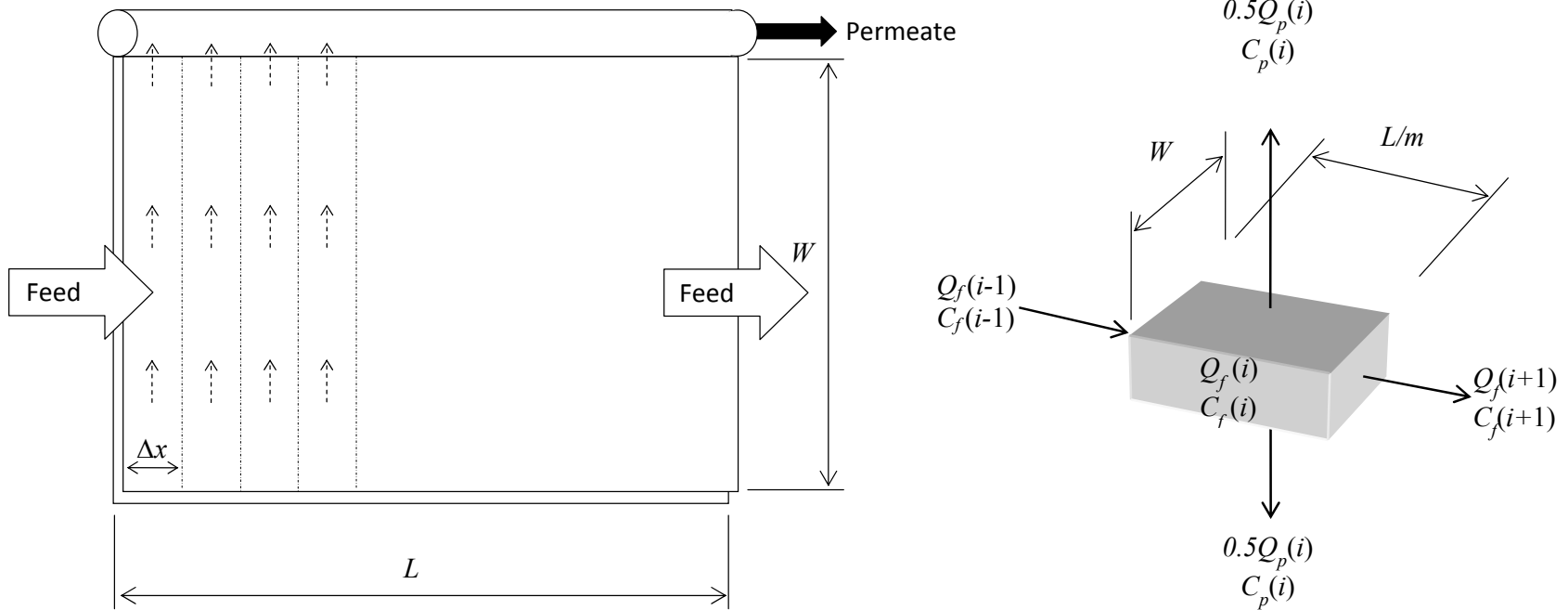
502 **Figure 6:** Observed and modelled overall rejection of NDMA, NMEA and NDEA (feed  
503 solution contains 20 mM NaCl, 1 mM NaHCO<sub>3</sub>, 1 mM CaCl<sub>2</sub>; feed temperature = 20.0 ±  
504 0.1 °C).

505 **Figure 7:** Overall rejection of N-nitrosamines by the pilot-scale experiments (overall  
506 permeate flux = 10, 20 and 30 L/m<sup>2</sup>h; feed solution contains 20 mM NaCl, 1 mM NaHCO<sub>3</sub>,  
507 and 1 mM CaCl<sub>2</sub>; feed temperature = 20.0 ± 0.1 °C). Open symbols indicate that the permeate  
508 concentration was below the instrumental detection limit. Values reported here are the  
509 average and ranges of duplicate results.

510 **Figure 8:** Effects of recovery on the rejection of NDMA, NMEA and NPYR (feed solution  
511 contains 20 mM NaCl, 1 mM NaHCO<sub>3</sub>, and 1 mM CaCl<sub>2</sub>; feed temperature = 20.0 ± 0.1 °C).

512 **Figure 9:** Variation in (a) feed pressure, (b) local permeate flux, (c) NDMA rejection and (d)  
513 NDMA concentration in the feed and permeate (feed solution contains 20 mM NaCl, 1 mM  
514 NaHCO<sub>3</sub>, and 1 mM CaCl<sub>2</sub>; feed temperature = 20.0 ± 0.1 °C).

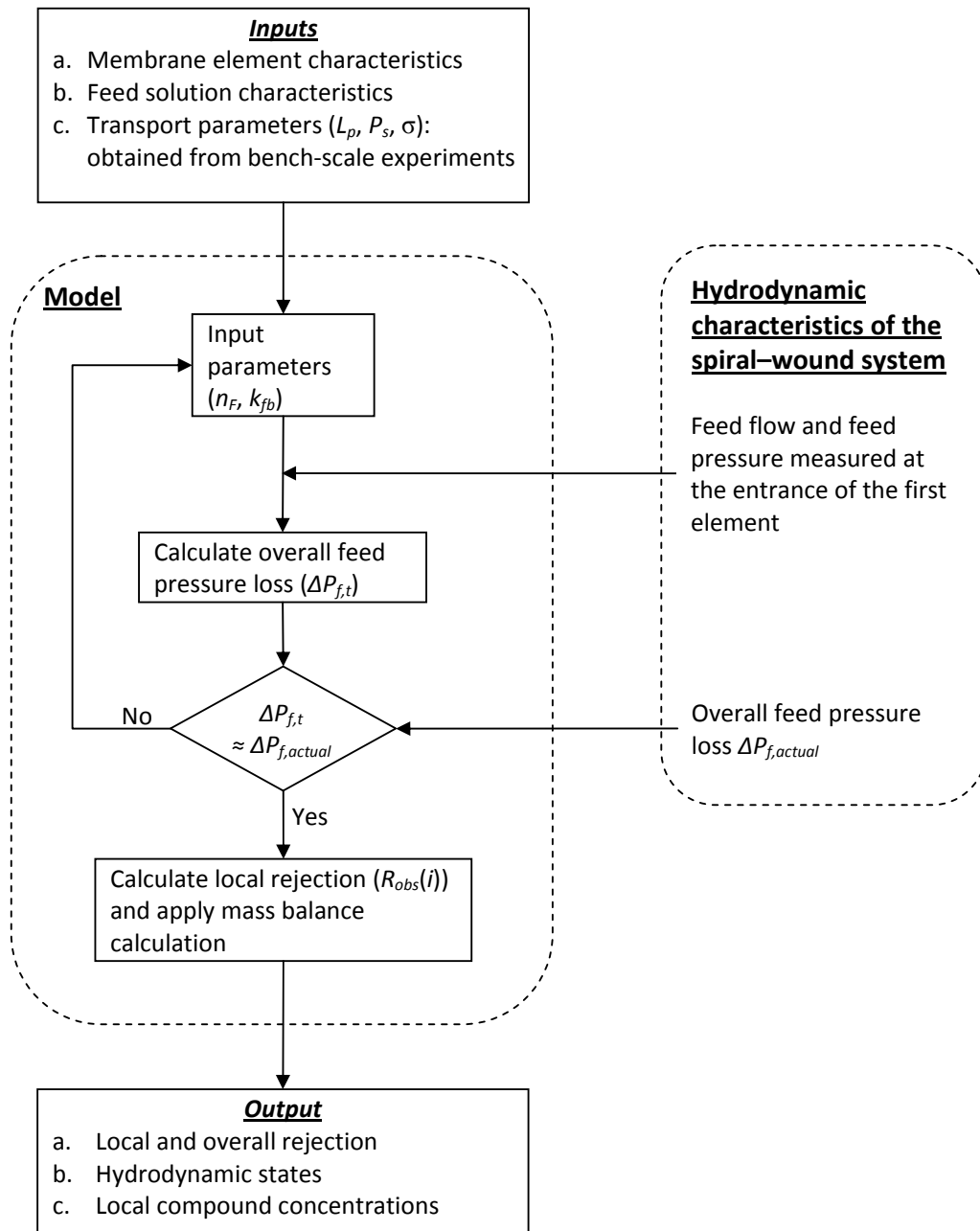
515



516

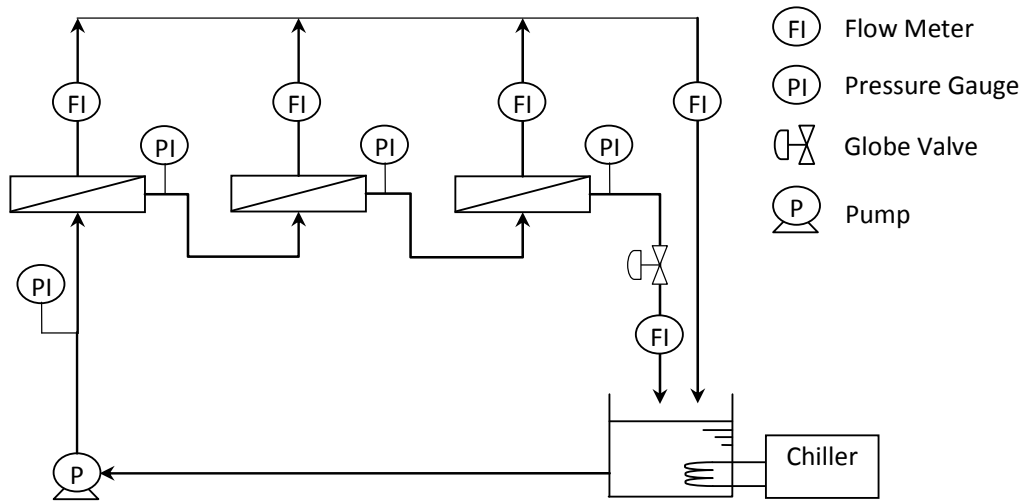
517 **Figure 1**





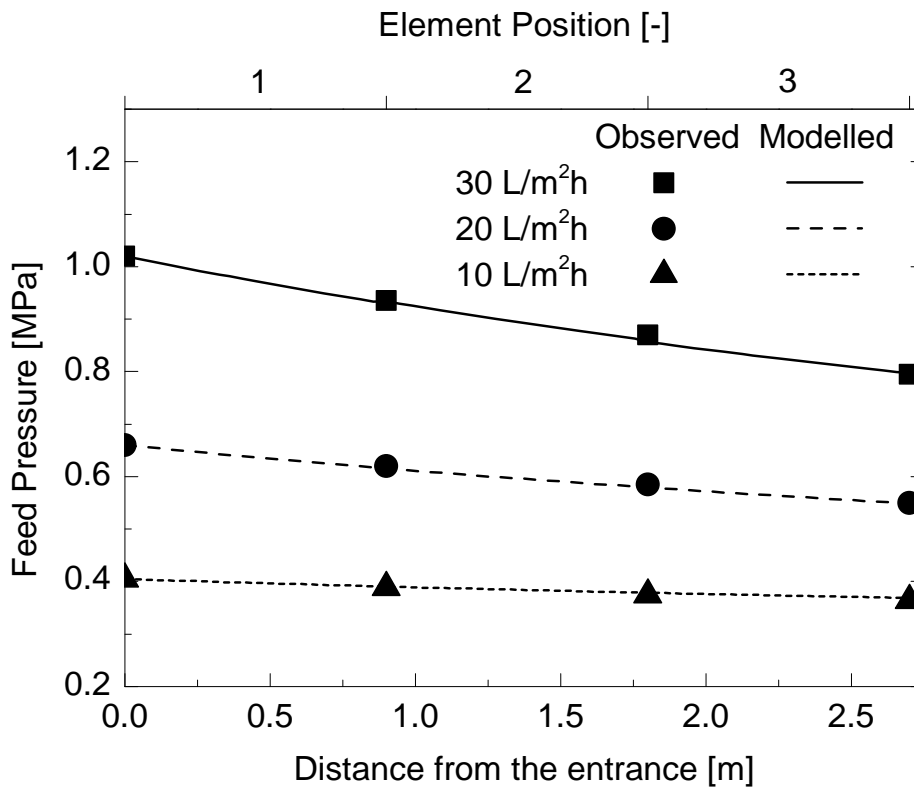
518

519 **Figure 2**



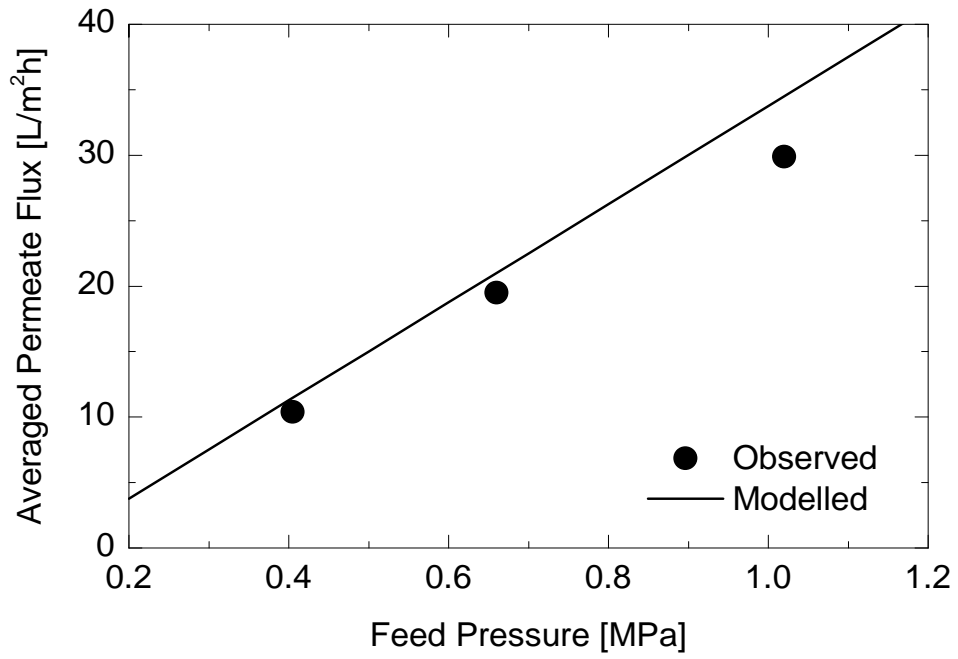
520

521 **Figure 3**



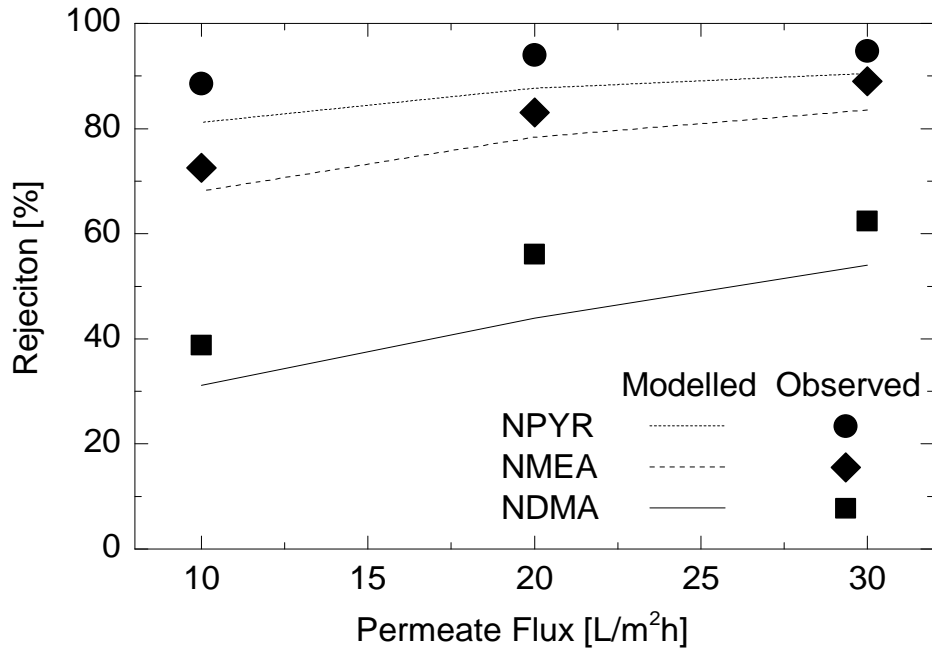
522

523 **Figure 4**



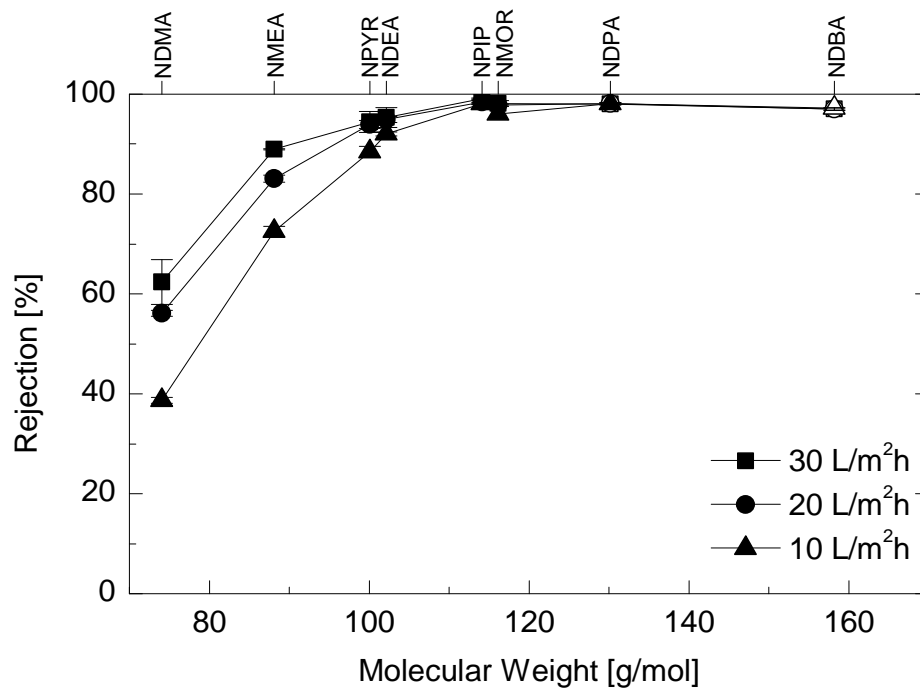
524

525 **Figure 5**



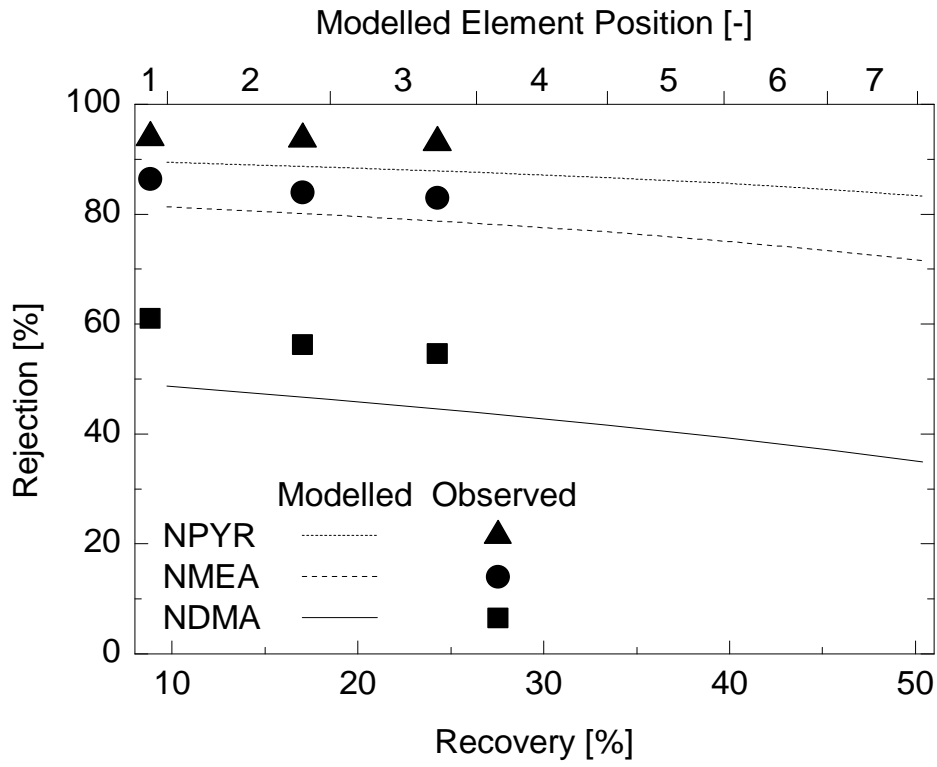
526

527 **Figure 6**



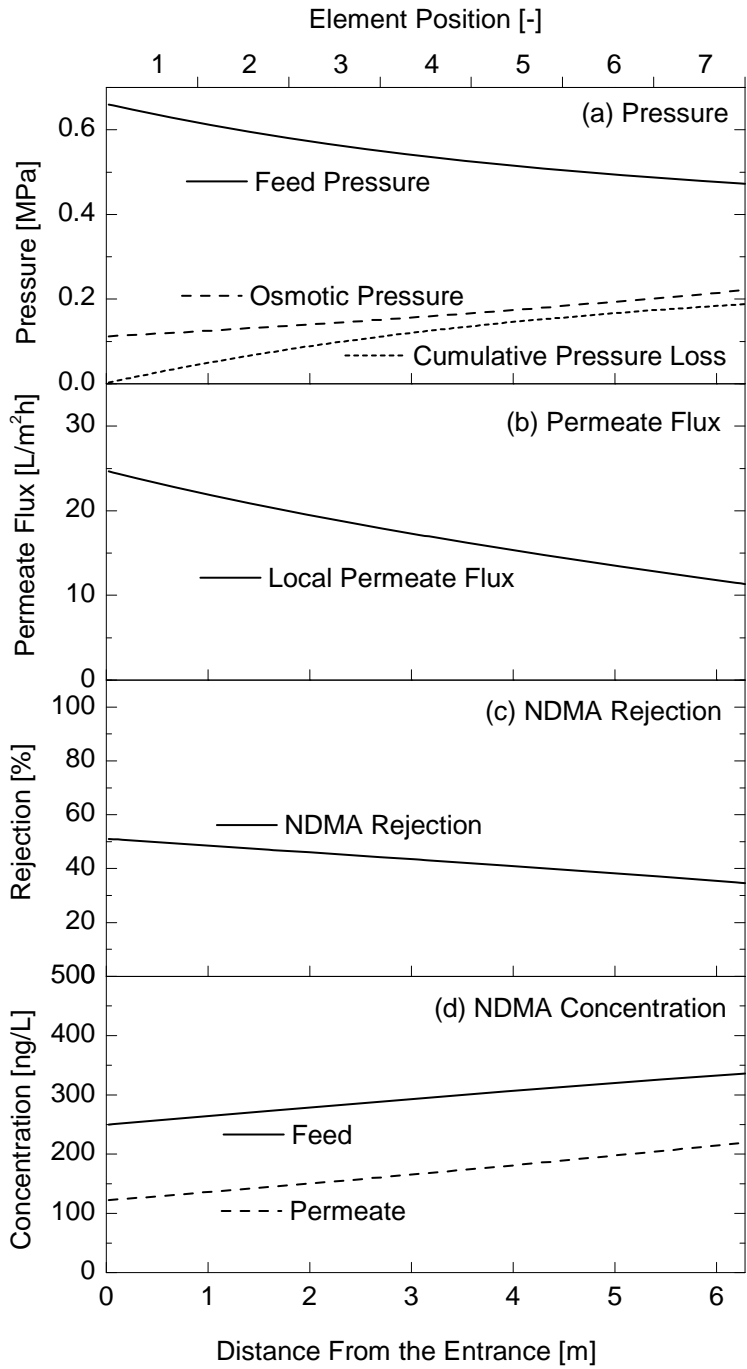
528  
529

**Figure 7**



530

531 **Figure 8**



532  
533 **Figure 9**